

**NEW PROCESS OF DEVELOPING NANOCRYSTALLINE FeCr
FOR FUEL CELL APPLICATION**

Ketua penyelidik: Prof. Madya Mohd. Ashraf Bin Othman

**Ahli penyelidik: Prof. Dr. Ing. Ir. Darwin Sebayang
Prof. Sulaiman bin Hj. Hasan
Dr. Ing. Pudji Untoro
Dr. Mat Husin Bin Saleh
Tjipto Sujitno
Deni Shidqi Khaerudini
Hendi Saryanto
Egi Agustian
Dafit Feriyanto**

**GERAN PENYELIDIKAN FUNDAMENTAL RESEARCH GRANT SCHEME
NO. VOT. 0759**

UNIVERSITI TUN HUSSEIN ONN MALAYSIA

ABSTRACT

The objectives of this study are to explore the high energy ball milling combined with ultrasonic treatment to develop smaller crystallite size, finer surface morphology, higher thermal stability and more homogenous nanocrystalline $\text{Fe}_{80}\text{Cr}_{20}$ alloys. The process that combined both is not fully investigated. They are carried out by high energy ball milling with milling time of 60 h and ultrasonic treatment using frequency of 35 kHz at various period of 3 h, 3.5 h, 4 h, 4.5 h, and 5 h. Characterization was carried out to all sample by X-Ray Diffraction (XRD), Scanning Electron Microscope (SEM) and Energy dispersive X-ray Diffraction (EDS), Thermo Gravimetric Analysis (TGA) and Particle Size Analyzer (PSA). The result showed that the combination process (milling combined with ultrasonic technique/named of milled and UB) samples effectively increased the solid solubility of Cr to Fe up to 62.1% and decreased the crystallite size to 2.71 nm at milled and UB 4.5 h, and have finer surface structure. Composition of combination samples are at suitable composition of 20.05 wt% Cr and 79.95 wt% Fe compared with raw material, ultrasonic treatment (UB) samples and milled 60 h sample. Lower gradation is observed on combination sample at 1100 °C up to 12.7 mg/ 52 wt%, 48 wt% and 25 wt% which is compared with $\text{Fe}_{80}\text{Cr}_{20}$ as raw material, UB samples and milled 60 h sample, respectively. The particle size decreased up to 5.23 μm and particle size distribution of combination process relatively increased up to 89.57% compared with UB samples, and milled 60 h sample.

ABSTRAK

Objektif kajian ini adalah untuk meneroka bola penggilingan tenaga tinggi digabungkan dengan ultrasonic untuk mengembangkan menghaluskan ukuran kristal, menghaluskan morfologi permukaan, menstabilkan habayang lebih tinggi dan mendapatkan paduan yang lebih homogeny nanokristalin $Fe_{80}Cr_{20}$ serbuk aloi. Gabungan proses masih terhad diselidiki. Dalam kajian ini tenaga yang tinggi pada bola penggilingan digunakan dengan masa penggilingan 60 h dan perlakuan ultrasonic dengan frekuensi 35 kHz pada perbezaan masa iaitu 3 h , 3.5 h , h , 4.5 h , dan 5 h . Kajian terperinci telah dijalankan untuk semua sampel oleh X -Ray Belauan (XRD), Mikroskop Imbasan Elektron (SEM) danTenaga serakan X -ray Belauan (EDS), Thermo Gravimetric Analisis (TGA) dan Saiz Zarah Analyzer (PSA). Hasilnya menunjukkan bahawa proses gabungan (penggilingan digabungkan dengan teknik ultrasonik/dinamakan daripada gilingan dan UB) sampel efektif meningkatkan kelarutan pepejal Cr untuk Fe sehingga 62.1 % dan mengurangkan saiz kristal sehingga 2.71 di gilingan dan UB 4.5 h dan meningkatkan kehalusan struktur permukaan. Komposisi sampel proses kombinasi menunjukkan bahawa komposisi 20 % berat Cr dan 80 % berat Fe telah dihasilkan. Penggredan Rendah dipelihara pada sampel gabungan pada $1100^{\circ}C$ sehingga 12.7 mg / 52 wt %, 48 % berat dan 25 % berat yang berbanding $Fe_{80}Cr_{20}$ sebagai bahan mentah, sampel perlakuan ultrasonic (UB) dan gilingan 60 h sampel, masing-masing. Saiz zarah dikurangkan sehingga 5.23 μm dan saiz zarah pengedaran gabungan proses meningkat sehingga 89.57 % berbanding gilingan 60 h sampel UB.

TABLE OF CONTENT

TITLE	i
PREFACE AND DEDICATION	iii
ACKNOWLEDGMENT	iv
ABSTRACT	v
TABLE OF CONTENT	vii
LIST OF TABLES	xi
LIST OF FIGURES	xiii
LIST OF SYMBOLS AND ABBREVIATION	xvii
CHAPTER 1 INTRODUCTION	
1.1 Research background	1
1.2 Problem statement	3
1.3 Hypothesis	4
1.4 Research objectives	4
1.5 Scope of study	5
1.6 Expected result	6
CHAPTER 2 LITERATURE REVIEW	
2.1 Introduction of SOFC	7
2.1.1 SOFC Material	8
2.1.2 Crystal structure for solid oxide fuel cell (SOFC)	9
2.1.3 Operating Principle of SOFC	11
2.1.4 SOFC component	13
2.1.4.1 Anode	13
2.1.4.2 Cathode	15
2.1.4.3 Electrolyte	17

2.1.4.4	Interconnection	18
2.2	Oxidation of metallic alloy	20
2.3	Metallic interconnect	21
2.3.1	Chromium based alloys	24
2.3.2	Iron based alloys	25
2.3.3	Iron-Chromium Alloys	27
2.4	Mechanical alloying	30
2.4.1	Control agent in ball milling process	31
2.4.2	Temperature of ball milling	31
2.4.3	Temperature increase during ball milling process	32
2.4.4	Ball milling mechanism	33
2.4.5	Ductile-ductile Fe and Cr sample	36
2.4.6	Solid solubility	37
2.4.7	Intermetallic synthesis	38
2.5	Nanocrystalline	39
2.6	Effect of crystallite size	42
2.7	Determining crystallite size	44
2.7.1	Measuring interplanar spacing and lattice parameter	45
2.7.2	Measuring solid solubility	46
2.7.3	Measuring $B_{corrected}$	47
2.7.4	Measuring crystallite size and strain of the material	49
2.8	Particle size and distribution	50
2.9	Ultrasonic technique	52
2.9.1	Maximizing the cavitations	54
2.9.2	Mechanism of ultrasonic technique	55
2.9.3	Broader application area for ultrasonic technique	56
2.10	Summary of literature review	57

CHAPTER 3 METHODOLOGY

3.1	Sample designation	60
3.2	Flow chart	61

3.3	Starting material	63
2.3	Powder blending	63
2.5	Sonification Process	67
2.6	Combination treatment	68
2.7	Characterization	71
2.7.1	X-Ray diffraction analysis	71
2.7.2	Morphology characterization	72
2.7.3	Thermal analysis	74
3.7.4	Determining particle size and distribution	76

CHAPTER 4 RESULT AND DISCUSSION

4.1	XRD pattern analysis	79
4.1.1	XRD pattern of raw material ($\text{Fe}_{80}\text{Cr}_{20}$)	80
4.1.2	XRD pattern of the ultrasonic treatment (UB) samples and raw material	81
4.1.3	XRD peaks of the milled 60 h and combination (milled and UB) Samples	83
4.1.4	XRD pattern of treated and untreated samples	85
4.2	Determining crystallite size using Williamson-Hall method	86
4.2.1	Crystallite size and strain of the raw material and the ultrasonic (UB) samples	88
4.2.2	Crystallite size and strain of the milled 60 h and combination (milled and UB) samples	91
4.2.3	Comparison crystallite size and strain of the treated and untreated samples	94
4.3	The relation between lattice parameter and the solid solubility	97
4.4	Surface morphology of the treated and untreated samples	99
4.4.1	Surface Morphology of Cr and Fe powder as raw materials	100
4.4.2	Surface morphology of ultrasonic (UB) powders	101

4.4.3	Surface morphology of milled 60 h and combination (milled and UB) samples	103
4.5	Identification of the chemical composition	105
4.6	Determining the thermal stability	108
4.6.1	Thermal stability of the UB samples	108
4.6.2	Thermal stability of the milled 60 h samples and combination samples	110
4.6.3	Comparison thermal stability of treated and untreated samples	111
4.7	Particle size and distribution of the treated and untreated samples	114
4.8	Summaries of the results	116
 CHAPTER 5 CONCLUSIONS AND RECOMMENDATIONS		
5.1	Conclusion	119
5.2	Recommendations	120
 REFERENCE		
APPENDIX A	XRD analysis	136
APPENDIX B	SEM analysis	150
APPENDIX C	PSA analysis	165
APPENDIX D	TGA analysis	184

LIST TABLE

Table 2. 1	SOFC materials properties within several operation temperature	9
Table 2. 2	Atomic radius and crystal structures for 16 metals	11
Table 2. 3	Advantages and disadvantages of several type anode material	13
Table 2. 4	Advantages and disadvantages of several type cathode material	15
Table 2. 5	Advantages and disadvantages of several type electrolyte material	17
Table 2. 6	Advantages and disadvantages of several types interconnect material	19
Table 2. 7	Varies metallic candidate material for interconnect application	23
Table 2. 8	Properties of chromium powder	24
Table 2. 9	Chemical properties of iron powder	26
Table 2. 10	Temperature rise during ball milling process	33
Table 2. 11	Varies effect of the crystallite size of the metallic and ceramic material	44
Table 3. 1	Samples designation	60
Table 3. 2	Detail information of raw material	63
Table 3. 3	Various diameter and amount of ball mill	64
Table 3. 4	Technical data of ultrasonic bath machine	68
Table 3. 5	The ball milling and ultrasonic of the previous research	69
Table 3. 6	Specification of particle size analyzer (PSA) machine	78
Table 4.1	XRD data of the Fe ₈₀ Cr ₂₀ alloys powders	80
Table 4.2	Result of XRD analysis of the treated and untreated samples	87
Table 4.3	Crystallite size and strain of the sample with ultrasonic bath treatment	89

LIST OF FIGURES

Figure 2.1	Configuration for planar design SOFC	8
Figure 2.2	Unit cell of crystal structure	10
Figure 2.3	Operating Concept of a SOFC	12
Figure 2.4	Anode with Ni-YSZ material	14
Figure 2.5	Cathode with LaMnO ₃ material	16
Figure 2.6	Temperature dependence of conductivity for undoped and Sr-doped LaMnO ₃	17
Figure 2.7	Phase diagram of Fe-Cr system	28
Figure 2.8	Oxidation in air of a Fe 26 wt% Cr 1 wt% Mo alloy	29
Figure 2.9	Grain size vs milling time for CoZr	32
Figure 2.10	Collision of the powder when mixture during mechanical alloying	34
Figure 2.11	Particle size distribution at various ball milling times under steady-state conditions	35
Figure 2.12	Refinement of particle and grain sizes with milling time	36
Figure 2.13	Deformation characteristic of starting powder in ball milling process	37
Figure 2.14	Schematic diagram of solid solubility vs milling	37
Figure 2.15	Solid solubility of Fe in Cu	39
Figure 2.16	Classification of nanocrystalline materials	40
Figure 2.17	Volume fractions of the crystallite, grain boundary, triple line and quadruple node as a function of crystallite size	41
Figure 2.18	Grain size and hardness of a ball milled Fe ₂₀ Cr alloy versus annealing time at 600 ⁰ C	43
Figure 2.19	X-Ray Diffraction	46
Figure 2.20	FWHM of the standard reference material for LaB ₆ on an in-house Cu K α diffractometer	48
Figure 2.21	Principle of the laser diffraction	51

LIST OF SYMBOLS and ABBREVIATION

SOFC	- Solid Oxide Fuel Cell
SO _x	- Sulfur Oxide
NO _x	- Nitrogen Oxide
CO ₂	- Carbon Dioxide
CO	- Carbon Monoxide
CH ₄	- Methane
rad	- radian
H ₂	- Hidogen
μm	- Mikro Meter (10 ⁻⁶ meter)
nm	- nano meter (10 ⁻⁹ meter)
YSZ	- yttrium stabilized zirchonia
LaMnO ₃	- Lanthanum Manganite
Ni	- Nickel
H ₂ O	- Air
Fe	- Iron
FeO	- Iron oxide
Cr	- Chromium
CO ₂	- Carbon dioxide
Fe-Cr	- Iron Chromium alloy
Cr ₂ O ₃	- Chromium Oksida
BCC	- Body Centered Cubic
FCC	- Face Centered Cubic
HCP	- Hexagonal Close-Packed
Å	- Angstrom
D	- The diameter crystallite size (nm).
K	- The shape factor (K=0.9).
λ	- Wavelength of the X-Ray (λ=0.154056 nm for Cu-K α).

CHAPTER 1

INTRODUCTION

This chapter consists of the research background, problem statement, hypothesis, research objectives and scope of study.

1.1 Research Background

Solid Oxide Fuel Cells (SOFC) research develop most interest currently as its potential to create an efficient system, high energy-density power generation device which typically operates at high temperatures relatively ($\cong 1000^{\circ}\text{C}$). Interconnection required to connect thermally the different cells and also provides the physical barriers to keep the oxidant and fuel separated (Yaodong *et al.*, 2007). There is high interest in nanocrystalline iron and chromium based alloys. The iron-chromium system has long been used by many engineering alloys as the basis in high-strength and corrosion-resistant applications, such as for fuel cell interconnect. Traditionally, iron-based alloy with additions of chromium has been used as high temperature (up to 1000°C) applications (Basu, 2007), where the stabilization and oxidation behavior at high temperature are fundamental in actual applications. Chromium has a phase stabilizer when added into the iron. It is because the chromium has the same BCC crystal structure and made primarily to promote the formation of a dense, adherent layer of Cr_2O_3 on the surface of the alloy (Craig, 1995).

Developing $\text{Fe}_{80}\text{Cr}_{20}$ based alloy using mechanical alloying via high energy ball milling was successfully carried out by Saryanto, *et al.*, (2008). Mechanical alloying (MA) are in general micro and nano structured often have remarkable properties. The product depends on many parameters such as the milling conditions, amount material which are being processed, type of the ball mill used, and milling time (Suryanarayana, 2001; Suryanarayana, 2004). Mechanical alloying technique is

able to synthesize single-phase FeT (T = Cr, Cu and Ni) binary alloys with average crystalline size below 50 nm and exhibiting a variety of magnetic responses (Martínez-Blanco *et al.*, 2011). Therefore, it is very challenging to develop nanocrystalline FeCr alloy, because the Cr metal encourage the formation of protective oxide (scale) (Quadackers *et al.*, 2003). Nanoscale particle research has become a very important field in materials science recently. A nanocrystalline material was characterized by a microstructural length scale in 1 to 100 nm range (Koch, 2003). Nano powders / nano materials with physical, chemical, and the mechanical properties can be utilized as the main building of innovative solutions for the problems in energy, environment, health and communication (Ozlem *et al.*, 2012). Nanoscale particles usually have different physical properties compared with large particles. It had been found that nanoparticles exhibit variety of previously unavailable properties including magnetic, optical, and other physical properties as well as the surface reactivity depend on particle size (Poole *et al.*, 2003). Therefore, heat-resistant nanoscale particle alloys was produced in the industrial scale and widely used in different fields of science and technology.

In the area of ultrasonic processing in liquid media, the development of the power generators family with extensive radiators has strongly contributed to the implementation at semi-industrial and industrial stage of several commercial applications. Some of the applications are in food industry, environment, process for manufacturing, etc. (Juan *et al.*, 2010). The use of high-intensity ultrasonic enhances the reactivity of metals as stoichiometric reagents became an important synthetic technique for many heterogeneous organic and organometallic reactions, especially for the involving reactive metals. In particular for small matter from several nanometers on couple of microns, ultrasonic is very effective in breaking agglomerates, aggregates and even primaries (Thomas *et al.*, 2006; Pudji *et al.*, 2009; Krisztian *et al.*, 2010; Darwin *et al.*, 2010a). The mechanism of the rate enhancements in reactions of metals had been done by monitoring the effect of ultrasonic vibration on the kinetics of chemical reactivity of solids, examining the effects of vibration on the surface morphology and size distributions of powders (Suslick, 1994; Kenneth *et al.*, 1999; Pudji *et al.*, 2009; Darwin *et al.*, 2010a). Ultrasonic treatment also effectively refines the surface morphology on FeCrAl substrate (Yanuandri, 2011; Ade, 2012). However, the exploration and improvement

novel processes enhance the reducing of finer crystallite size and homogenous distribution crystalline size of iron-chromium is still very challenging.

Many researchers field investigate the nano material using ball milling and ultrasonic technique in mixing raw material (Suryanarayana, 2001; Quadakkers *et al.*, 2003; Suryanarayana, 2004; Saryanto, *et al.*, 2008; Pudji *et al.*, 2009; Darwin *et al.*, 2010a; Ade, 2012; Ozlem *et al.*, 2012). However, unsatisfactory performance still resulted when applied at high temperature operation such as grain growth, rough surface morphology, high oxidation, and the composition not appropriate with working composition. Study using combination treatments between ball milling and ultrasonic technique have not yet been investigated. This study focus on the development of iron-chromium powder promoted using combination treatment in order to achieve smaller crystallite size, finer the surface morphology, more homogenous and better thermal stability of Fe₈₀Cr₂₀ alloys powder.

1.2 Problem statement

The challenge in this research is how to produce the nano range crystallite size, finer surface morphology, high thermal stability and homogenizing powders size. Ball milling process is significant to reduce the crystallite size into nano range size. Nevertheless, since processing techniques involves high-temperature conditions at longer processing times is inevitable (Suryanarayana, 2001; Suryanarayana, 2003; Quadakkers *et al.*, 2003; Suryanarayana, 2004). In previous research, growth rate from 5.82 nm to 38.51 nm occurred (Hendi, 2011; Deni, 2011). Meanwhile, Ultrasonic process with fixed frequency develop and achieve the not homogenous and finer grain structure alloys powder (Suslick, 1988; Kenneth *et al.*, 1999; Mikko *et al.*, 2004; Thomas Hielscher, 2005; Darwin *et al.*, 2010a; Ade, 2012; Pudji *et al.*, 2009). According to Yanuandri, (2011); Ade, (2012), the frequency was conducted in 18.52 kHz and holding time of 10, 20, and 30 minutes which were obtained the rough surface and less homogenous. Nanoscale material have many advantages when compared with large particle. It was proved by Hendi (2011) and Deni (2011) that the commercial ferritic steel some cracks was observed on the consolidated

specimen. It means that large particles have low thermodynamic stability when consolidated at a temperature of 900 °C and above. Therefore, smaller grain size, finer surface morphology and more homogeneous crystallite sizes in the nano range size are required in operation at high temperatures.

1.3 Hypothesis

The hypotheses considered in this research are:

1. Ball milling time of 60 hours with the ratio of the ball to the powder is about 1:13 will be most effective to reduce the powder size into nanometer range size.
2. Ultrasonic technique with the longer ultrasonic times will improve the homogeneous and finer surface morphology.
3. Combination treatment of ball milling and ultrasonic will develop new Fe₈₀Cr₂₀ alloy powder which has smaller crystallite size, more homogeneous, finer surface morphology and higher thermal stability.

1.4 Research objectives

Research objectives in this study are to explore the high energy ball milling combined with ultrasonic technique to develop smaller crystallite size, finer surface morphology, higher thermal stability and more homogeneity of nanocrystalline Fe₈₀Cr₂₀ alloys can improve the properties. The sub-objectives:

- i. To develop nanostructured Fe₈₀Cr₂₀ alloy by using ultrasonic technique, ball milling and combination treatment (milled combined with ultrasonic technique).
- ii. To investigate the different ultrasonic time in improving uniform fine grain of nanostructured material.

- iii. To investigate combination treatment (milled combined with ultrasonic) to reduce powder size, uniform fine grain, finer surface morphology and high thermal stability.

1.5 Scope of study

The scope of this research includes:

1. Composition material alloy of 80 wt% Fe, and 20 wt% Cr.
2. Developing the $\text{Fe}_{80}\text{Cr}_{20}$ nanostructure alloy by using ball milling process with milling time of 60 hours.
3. Only gas nitrogen is use in high energy ball milling process
4. Ultrasonic process will be introduced at appropriate high frequency of 35 kHz and holding time 3 h, 3.5 h, 4 h, 4.5 h, and 5 h.
5. Assumed the pressure of the open environment when ultrasonic process is 1 atm.
6. Study the effect of crystallite size $\text{Fe}_{80}\text{Cr}_{20}$ alloy powder after ultrasonic process, milling process and combination process.
7. Study the effect of ultrasonic process on the fine surface morphology and homogenous alloy powder.
8. Study the distribution of particle size and thermal stability after ultrasonic process, milling process and combination process.
9. Analysis of the microstructure and grain size by using Scanning Electron Microscopy (SEM).
10. Phase analyses by using X-Ray Diffraction (XRD).
11. Thermal analysis by using Thermo Gravimetric analysis (TGA) with temperature of 1100 °C which are carried out to the all samples (treated and untreated samples).
12. Determine particle size and the distribution of particle size by using Particle Size Analyzer (PSA).

1.6 Expected result

Ball milling process using optimum milling time is expected to improve the physical properties of the nanostructure alloy powders. Moreover, the vibration of the ultrasonic machine through the frequency is expected to be effective for breaking agglomerates. Compared to those treatments, the combination of both treatments (combination treatment) is expected to obtain the smaller crystallite size, more homogenous, finer surface structure, higher thermal stability, higher strain and higher solid solubility of $\text{Fe}_{80}\text{Cr}_{20}$ alloy powder can be developed.

CHAPTER 2

LITERATURE REVIEW

This chapter explains the literature review which related with the research. It consists of the theory about Solid Oxide Fuel Cell (SOFC), interconnect, developing nanocrystalline material, homogenizing, and refining the surface morphology.

2.1 Introduction of SOFC

According to Zhang (2006), Solid Oxide Fuel Cell (SOFC) is a promising technology for electricity generation. It converts the chemical energy of the fuel gas to electrical energy directly. Therefore, the electrical efficiencies can be achieved through this system. The system can reach efficiency approximately 80% (efficiency of internal combustion engine is no more 40%) when couple it with heat recovering system for cogeneration (heating applications and electric power). Besides, SOFC can replace several of fuels and widely implemented to power supplies from small-scale distribution power supplies to large-scale thermal power generation (Blein, 2005).

2.1.1 SOFC Material

The structure of SOFC is well stacked which consists of anode, electrolyte, cathode, and interconnect materials as in Figure 2. 1 (Quadackers, 2003). Besides, the material properties for SOFC component in various temperatures are tabulated in Table 2.1.

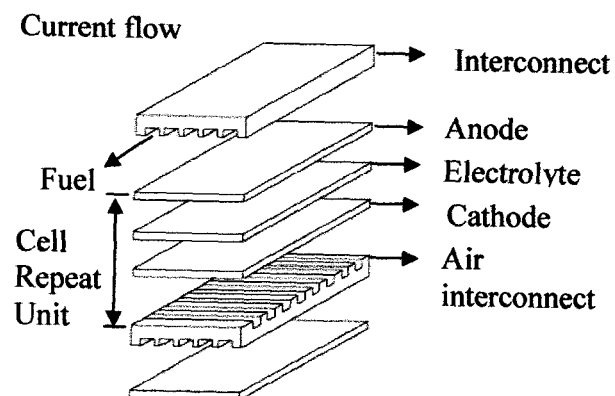


Figure 2. 1 Configuration for planar design SOFC (Singhal, 2000)

There are many types of materials for SOFC components which are applied by researcher to develop the efficient SOFC system. The most materials which are used in the SOFC components and its depend on the temperature application as listed in the Table 2. 1:

1. Electrolyte : Yttrium Synchronize Zirconia (YSZ), Scandia Stabilized Zirconia (SCZ), Lanthanum Strontium Gallium Magnesium (LSGM), and Cerium Gadolinium Oxide (CGO).
2. Cathode : Lanthanum Strontium Manganite (LSM) and $\text{La}_{0.6}\text{Sr}_{0.4}\text{Co}_{0.2}\text{Fe}_{0.8}\text{O}_3$ (LSCF).
3. Anode : Nickel-Yttria Stabilized Zirconia (Ni-YSZ) and Nickel-Samaria Doped Ceria (NI-SDC).
4. Interconnect : Lanthanum Chromites/ LaCrO_3 (LCR), Ferritic steel and stainless steel.

Table 2. 1 SOFC materials properties within several operation temperatures (Rajendra, 2007)

SOFC operating temperature (°C)	Material				Cell design	Electrolyte thickness (µm)
	Electrolyte	Cathode	Anode	Interconnect		
950-1000	YSZ	LSM	Ni-YSZ	LCR	Tubular	40
					Planar	150-300
650-800	YSZ, SCZ	LSM	Ni-YSZ	Ferritic steel	Planar	5-20
400-650	LSGM, CGO	LSCF	Ni-SDC	Ferritic steel	Planar	500 or less
				Stainless steel	Planar	5 (LSGM)
				Stainless steel	Planar	10-30 (CGO)

2.1.2 Crystal structure for solid oxide fuel cell (SOFC)

A crystalline material is one of atoms which are situated in a repeating or periodic array over large atomic distances. Long-range crystal is observed after consolidation the atoms. It will position itself in a repetitive three-dimensional pattern. (Figure 2. 2). All metals, many ceramic materials, and certain polymers form crystalline structures under normal solidification conditions (Smith, 2004).

Some of the properties of crystalline solids depend on the crystal structure of the material, the manner in which atoms, ions, or molecules are arranged spatially. There is a large number of the different crystal structure. The crystal structure has a various structure from simple structure to the complex structure. A unit cell is chosen to represent the symmetry of the crystal structure; where all of atom positions in the crystal may be generated by translations of the unit cell integral distances along each its edges. Thus, the unit cell is the basic structural unit or building block of the crystal structure

and defines the crystal structure by virtue of its geometry and the atom inside positions (Smith, 2004).

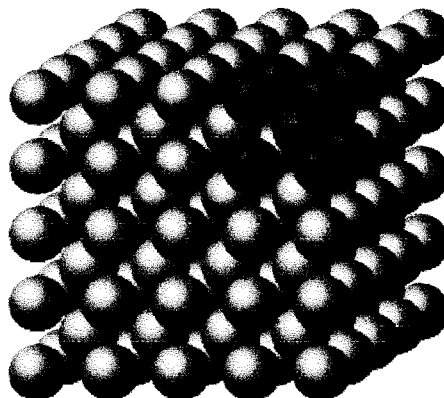


Figure 2. 2 Unit cell of crystal structure (Smith, 2004)

According to Seigo *et al.*, (2008) that the crystal structure of Fe-hydrogenase at 1.74 angstrom shows that the monocular iron is coordinated by cysteine sulphur of 176. The ligation pattern of the iron plays the essential role on the H₂ activation and it can to stimulate the catalyst synthesis which could substitute the platinum in fuel cell application.

Study of structural, electronic and magnetic behaviour of Cu_xFeCr_{1-x}O₂ has been investigated by Osman, (2013), they found that the partial crystal structure deformation from delafossite CrFeO₂ structure to corundum-type FeCrO₃ structure is containing of CrO₂ and Cr₂O₃ blocks. The crystal geometry is change when the Cr substitution was increased. Therefore, the FeCr based alloys used in this research in order to minimize the change of crystal geometry.

According to Qiu, (1998), that the FeCr in the CsCl (B₂) crystal structure has been studied. They found that in the antiferromagnetic phase the Fe and Cr sublattice has the unusual structure. In ferromagnetic and antiferromagnetic phase the Fe moment has decreased from that in pure BCC Fe and the Cr moment increased from that in pure BCC Cr.

Three simple crystal structures relatively are found for the most common metals which is listed in Table 2. 2: Face Cantered Cubic (FCC), Body-Cantered Cubic (BCC) and Hexagonal Close-Packed (HCP).

Table 2. 2 Atomic radius and crystal structures for 16 metals (Smith, 2004)

Metal	Crystal structure ^a	Atomic radius ^b (nm)	Metal	Crystal structure	Atomic radius(nm)
Aluminum	FCC	0.1431	Molybdenum	BCC	0.1363
Cadmium	HCP	0.1490	Nickel	FCC	0.1246
Chromium	BCC	0.1249	Platinum	FCC	0.1387
Cobalt	HCP	0.1253	Silver	FCC	0.1445
Copper	FCC	0.1278	Tantalum	BCC	0.1430
Gold	FCC	0.1442	Titanium (α)	HCP	0.1445
Iron (α)	BCC	0.1241	Tungsten	BCC	0.1371
Lead	FCC	0.1750	Zinc	HCP	0.1332

^aFCC (Face-Centred Cubic); HCP (Hexagonal Close-Packed); BCC (Body-Centred Cubic).

^bA nanometer (nm) equals m; to convert from nanometers to Angstrom units (Å), multiply the nanometer value by 10.

2.1.3 Operating Principle of SOFC

The cell is constructed with two porous electrodes with an electrolyte in the middle. Initially, the catalytically reaction can be described as follows, oxygen flows along cathode in order to contact among cathode and electrolyte interface for importing the ion oxygen to electrolyte and pass it towards anode. That reaction produces the water, carbon dioxide, heat, and the electrons (Gorte *et al.*, 2003). However, the electron flow will occur when the electrical connection between the cathode and the anode is established, where a continuous supply of oxygen ions (O^{2-}) generated from cathode to anode in order to maintain the overall electrical charge balance. Ultimately, this process produced the residual product pure water (H_2O) and heat. The operating of SOFC technology is shown in Figure 2.3.

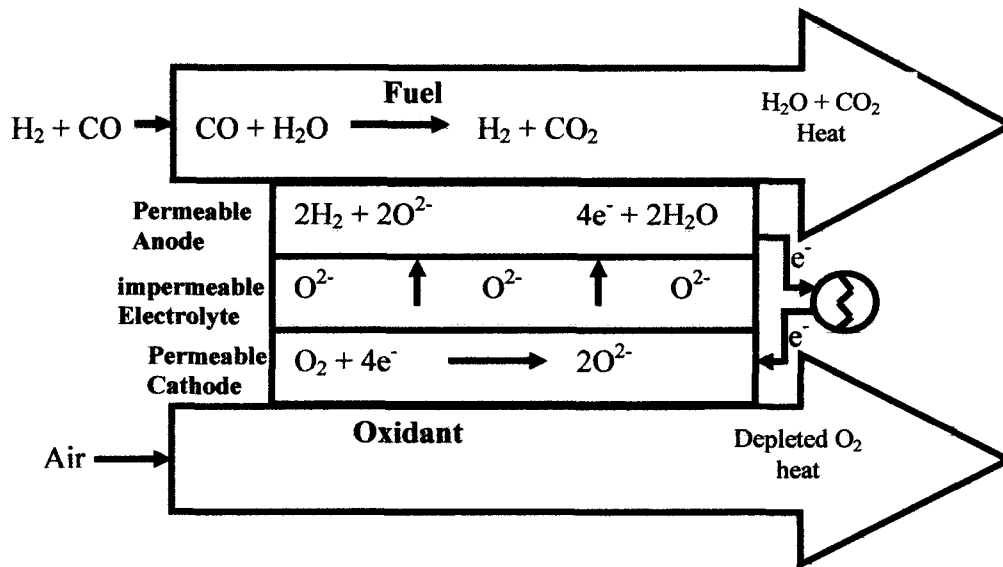


Figure 2.3 Operating Concept of a SOFC (Greneir *et al.*, 1995; EG&G, 2002; Benjamin, 2004; Michael *et al.*, 2006; Hendi, 2011)

In the real application, fuel cells are connected in a series of cells, in order to obtain higher outlet voltage. An interconnect plate is installed to provide the electronic contact between the anode of one cell and the cathode of the next cell (Navadol *et al.*, 2009).

Hydrogen, carbon monoxide (CO) and hydrocarbons such as methane (CH_4) can be used as fuels in SOFC system. The fuel stream reacts with oxide ions (O^{2-}) from the electrolyte to produce the water or CO_2 and to deposit electrons into the anode. The electrons pass outside fuel cell through the load and back to the cathode where oxygen from air receives the electrons and its converted into the oxide ions which is injected to the electrolyte (EG&G, 2002). At the temperature of $1000^\circ C$, the CO and CH_4 direct oxidation will occur. but it is less favoured due to the shift of the water gas from CO to H_2 and reforming from CH_4 to H_2 . (EG&G, 2002).

The electrochemical reactions in SOFC include:

At anode:



At cathode:



The overall cell reactions are:



2.1.4 SOFC Components

There are several components in SOFC system such as anode, cathode, electrolyte, and interconnect. All the components are described as follows.

2.1.4.1 Anode

Anode has developed by many engineers with different anode materials. Anode materials have a several types which have advantages and disadvantages as listed in Table 2. 3. The most commonly used as anode material is Ni-YSZ which described more detail.

Table 2. 3 Advantages and disadvantages of several type anode material (Zhang, 2006 and Gorte *et al.*, 2003 and Maarten, 2005)

No.	Types of anode material	Advantages and disadvantages
1	YSZ	Advantages: Offering the required oxygen vacancies for ionic conductivity Disadvantages: Ionic conductivity comes down significantly over time when working at high operating temperatures
2	Ni-YSZ	Advantages: Higher thermal expansion than YSZ, an

		<p>excellent catalyst for both steam reforming and hydrocarbon cracking, carbon deposition occurs rapidly when feeding hydrocarbons</p> <p>Disadvantages: Poor redox stability, low tolerance for sulphur and carbon deposition and the tendency of nickel agglomeration after prolonged operation</p>
3	SrTiO ₃	<p>Advantages: Low-cost raw materials and simple processing steps</p> <p>Disadvantages: The cubic to tetragonal structural phase transformation may induce strain or microcracks in a film grown on a SrTiO₃ substrate</p>

Anode has the smallest losses polarity if it is compared with other components, and as the layer that often provide mechanical support. The oxidation reaction between the oxygen and the hydrogen ions produce heat and water as well as electricity. One of the advantages of anode as the catalyst for steam reformer hydrocarbon gas becomes hydrogen fuel. It provides another operational benefit to the fuel cell stack due to the reforming cools stack reaction internally (EG&G,2002). Therefore, its material should be catalytic, conductive, as well as porous to hydrogen fuel. It may reduce the atmosphere and the thermal expansion must be compatible with the other cell. Ni-YSZ anode is currently the material of choice for anode material as shown in

Figure 2.4 (Singhal, 2000)

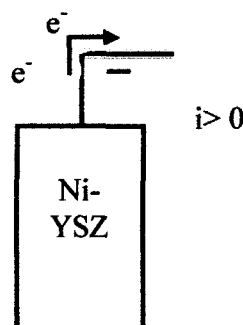


Figure 2.4 Anode with Ni-YSZ material (Singhal, 2000)

Most development has focused on Ni because of the abundance and affordability. However, Ni has a higher thermal expansion than YSZ ($13.3 \times 10^{-6} / \text{C}$ for Ni and $10 \times 10^{-6} / \text{C}$ for YSZ). Therefore, the Ni-YSZ composite was created. This is due to the YSZ

provides structural support for the separate Ni particles, preventing them from sintering together while matching thermal expansion. Adhesion of the anode to the electrolyte also increased (Singhal, 2003 and Zhong *et al.*, 2004).

2.1.4.2 Cathode

Cathode has developed by many engineers with different cathode materials. Cathode materials have a several types which have advantages and disadvantages as listed in Table 2. 4. The most commonly used as cathode material is LSM which described more detail.

Table 2. 4 Advantages and disadvantages of several type cathode material (Chunwen *et al.*, 2010; Hyo *et al.*, 2009)

No.	Types of cathode material	Advantages and disadvantages
1	LSM	Advantages: High electrical conductivity at higher temperatures, and its thermal expansion coefficient Disadvantages: increasing costs and longer start-up times
2	YSZ	Advantages: thermal insulator with high thermodynamic and chemical stability, low vacancy mobility, high ionic conductivity Disadvantages: increasing costs and longer start-up times
3	Gadolinia-Doped Ceria (GDC)	Advantages: high ionic conductivity and low cost production Disadvantages: lower operating temperatures (<700 °C)
4	Scandia Stabilized Zirconia (SCZ)	Advantages: high ionic conductivity, chemical stability and good electrochemical performance Disadvantages: there is a phase transition at 650 0 C from cubic to rhombohedral phase, lead to an abrupt change in volume and coefficient of thermal expansion (CTE) and thus cracking of the electrolyte material
5	Lanthanum Strontium Gallium	Advantages: high conducting properties at intermediate

	Magnesium (LSGM)	operating temperatures while providing stability Disadvantages: high thermal expansion
6	Samaria-doped Ceria (SDC)	Advantages: high ionic conductivity in the intermediate temperature range Disadvantages: high electrolyte resistance, hence degrade the performance.

The most commonly used cathode material is lanthanum manganite (LaMnO_3) as shown in Figure 2.5. Typically, it is doped with rare earth elements (eg. Sr, Ce, Pr) to enhance its conductivity.

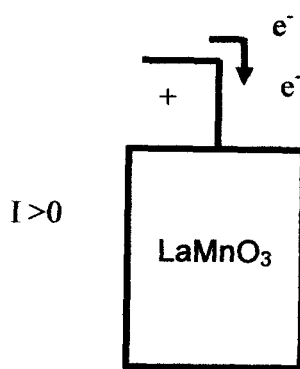


Figure 2.5 Cathode with LaMnO_3 material (Singhal, 2003)

The function of the crystal as electron is to conduct with no ionic conductivity. The electrons flow back through the open circuit of cathode cells to reduce molecular oxygen and flow it back to the electrolyte. In addition, to make it more effective in flowing the oxygen, it can be achieved through YSZ electrolytes material. It has adequate functionality at intermediate fuel cell temperatures (about $700\text{ }^\circ\text{C}$) and used with alternative electrolyte compositions (Zhang, 2006; Rajendra, 2007). Using electrolytes material can reduce operating costs and expand the materials selection, creating an opportunity for additional cost savings (Gorte *et al.*, 2003; Zhong *et al.*, 2004).

It has been found that by increasing the Sr^{2+} or Ca^{2+} content is possible to increase the electronic conductivity due to change in the Mn ratio (Chakraborty *et al.*, 1995). Its conductivity at $1000\text{ }^\circ\text{C}$ for $\text{La}_{0.8}\text{Sr}_{0.2}\text{MnO}_3$ varies in range of 100 to 200 S/cm which shows maximum value for a Sr-content close to 55 mol%. However, their ionic

conductivity are negligibly small, $\sim 10^{-7}$ S/cm at 800°C in air (Figure 2. 6). Therefore, this total conductivity (electronic and ionic) of LSM is not sufficient to completely neglect the in-plane resistance in the cathode. Besides, it is possible to minimize the corresponding losses by providing a larger geometry relatively and location of the current collector during cell operation (Sasaki *et al.*, 1999).

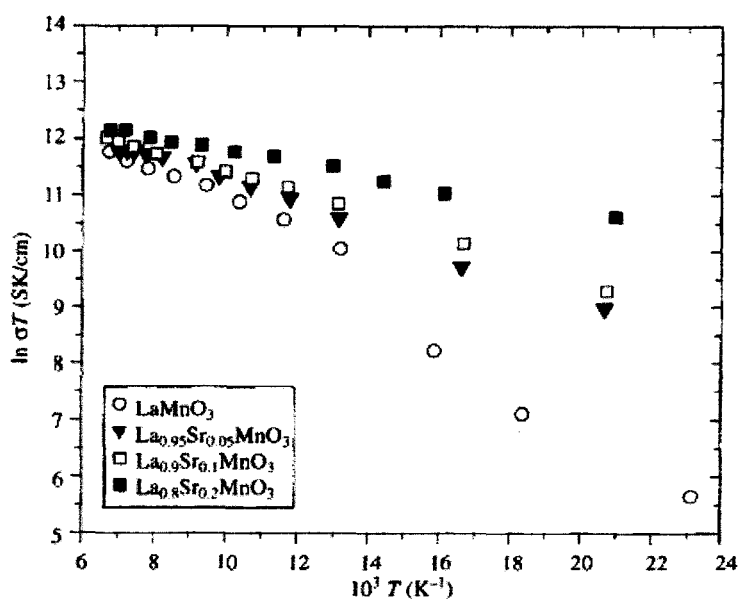


Figure 2. 6 Temperature dependence of conductivity for undoped and Sr-doped LaMnO₃ (Kuo *et al.*, 1990)

2.1.4.3 Electrolyte

Electrolyte has developed by many engineers with different electrolyte materials. Electrolyte materials have a several types which have advantages and disadvantages as listed in Table 2. 5. The most commonly used as electrolyte material is YSZ.

Table 2. 5 Advantages and disadvantages of several type electrolyte material (Wendy Lim, 2009; Crina *et al.*, 2009; Jennifer *et al.*, 2007)

No.	Types of electrolyte material	Advantages and disadvantages
-----	-------------------------------	------------------------------

1	YSZ	Advantages: Sufficiently high oxygen ion conductivity, suitable for tape casting, pellet pressing and other fabrication methods Disadvantage: Low oxygen conductivity
2	ScSZ	Advantages: High oxygen conductivity, suitable for tape casting, pellet pressing and other fabrication methods Disadvantage: High cost
3	Gadolinia-Doped Ceria (GDC)	Advantages: High ionic conductivity at intermediate operating temperatures, low cost, reduced ohmic losses, Disadvantage: Short circuiting and decreased power performance by electronic leakage
4	Lanthanum Strontium Gallium Magnesium (LSGM)	Advantages: High stability and ionic conductivity Disadvantage: high cost

The electrolyte conducts ionic charges to the electrodes and completes the cell electric circuit. It also provides a physical barrier to prevent the fuel and oxidant gas from mixing directly. Therefore, the electrolyte must possess a high ionic conductivity without electrical conductivity. To prevent gas from permeating one side of the electrolyte layer to another, it required impermeable material as an electrolyte and it also should be as thin as possible to minimize resistive losses in the cell (Zhang, 2006; Gorte *et al.*, 2003 and Zhong *et al.*, 2004).

2.1.4.4 Interconnection

Interconnect has developed by many engineers with different interconnect materials. Interconnect materials have a several types which have advantages and disadvantages as listed in Table 2. 6. The most commonly used as interconnect material is FeCr which described more detail.

Table 2. 6 Advantages and disadvantages of several types interconnect material (Minh, 1993; Sammes, 1997; Jeffrey, 2005; Junwei Wu and Xingbo Liu, 2010; Costa *et al.*, 2006; Redjald *et al.*, 2013; Sebayang *et al.*, 2013)

No.	Types of electrolyte material	Advantages and disadvantages
1	LSC ($\text{La}_{0.9}\text{Sr}_{0.1}\text{CrO}_3$)	Advantages: High Cr fraction, high Sr fraction, Disadvantages: Less conducting, expensive and difficult to fabricate as their brittleness
2	LaCrO_3 (LCR)	Advantages: stable in higher sintering temperature, Disadvantages: expensive and difficult to fabricate as their brittleness
3	Ca-doped yttrium chromite	Advantages: Better thermal expansion compatibility, especially in reducing atmospheres Disadvantages: Excess A-site element tend to react with zirconium electrolyte lead to produce undesirable secondary phases
4	FeCr	Advantages: High-strength and corrosion-resistant, high magnetic responses Disadvantages: Some grain growth at high temperature operation

The cell interconnection is exposed both of cathode and anode, so it must be stable chemically in both environments at 1000 °C. However, as a consequence for operating temperature of this material within high range, then the material should have fire resistance properties, oxidant gases, and proper coefficient of electronic conductivity (Zhang, 2006; Gorte *et al.*, 2003; Zhong *et al.*, 2004). One of approach promotes the formation of more conductive oxide phases could be accomplished by depositing thin films of certain metals onto the interconnect surface before oxidation. Upon heating, the metal coating oxidizes, reacts with the Cr from the base alloy, and subsequently forms another oxide layer than Cr_2O_3 (Jaing *et al.*, 2002; Tad *et al.*, 2005). Interconnect has a several vital function in SOFC system.

1. It provided electrical contact between allowing the stack to complete the function as a single power generation unit and provides mechanical support to the SOFC design (Benjamin, 2004).

2. It becomes physical barrier between repeating cells and interconnect which keep the oxidant and fuel gases from mixing by forming a dense (Benjamin, 2004).

Developing interconnect by many researchers with right material shown that its can improve the corrosion resistance at high temperature, protection in aggressive environments, high temperature coating, high temperature alloys and intermetallic, metal dusting and carburisation, role of water vapour and steam in high temperature corrosion, lifetime prediction spalling and advanced characterization techniques of degradation (Bastidas, 2006).

These three criteria are most important for interconnecting material such as high electrical conductivity, good stability in both condition reducing, oxidizing and matching for coefficient of thermal expansion (CTE) with other SOFC components (Benjamin, 2004). Ceramic interconnect such as doped lanthanum chromites ($\text{La}_{1-x}(\text{Sr,Ca})_x\text{CrO}_3$) have been widely used as interconnect material (Songlin *et al.*, 2008). These materials are expensive and difficult to fabricate as their brittleness. The reduction of SOFC operating temperature is possible to consider oxidation resistance metallic alloys. Metallic material is easier gained and interest replacement for the LaCrO_3 based ceramic (Geng *et al.*, 2006). Therefore, there are many researches develop Fe-Cr metallic material as interconnect SOFC application. FeCr powder alloy for interconnect SOFC application become challenge to improve the electrical conductivity (Khaerudini *et al.*, 2012), high corrosion resistance and decrease the growth rate which is provided by Cr_2O_3 scale (Deni, 2011). The Cr_2O_3 scale is suitable for resistance application such as for decrease the migration of chromium to SOFC cathodes and to defends a cell electrochemical performance (Hendi, 2011).

2.2 Oxidation of metallic alloy

Metal alloy had been became superior properties as compared with LaCrO_3 (traditionally material used for interconnect material) which offer potential to increase efficiency of

SOFC (Benjamin, 2004). The significant advantage of metallic interconnect, it can decrease resistance of the cell that would be directly convert into increased output and the electrical conductivity. It caused by the reduce temperature gradient within the structure that could give effect to stack efficiency of thermal stress (Benjamin, 2004; Minh, 1993). However, the metallic alloys have several negatives aspect for SOFC interconnect which are potential for adversely impacted during operation. It is due to thermal expansion mismatch between the other metal SOFC materials. Its Metal alloys have higher CTEs as compared to ceramic material. It is lead to significant level of stress developed when temperature changed. Metal is oxidized when exposed to the range of atmospheres and temperature during SOFC operation. Its efficiency was reduced due to higher surface resistance lead to excessive oxidation (Benjamin, 2004; Minh, 1993). Loss efficiency of the stack could due to oxidation of interconnect. It caused by increasing of electrical resistance of the oxidation layer. To improve the oxidation resistance is completed by addition of alloy and coating method (Kofstad, 1996; Benjamin, 2004). However, this study focuses on alloying addition process via new method.

2.3 Metallic interconnect

Metallic materials are easier and cheaper to fabricate, they are less brittle, easier for machining and they could be joined using a number of standard welding and brazing techniques. They have high thermal conductivities than ceramic materials (Deni, 2011 and Khaerudini *et al.*, 2012). The most important ability of metallic alloy is slow formation, thermal grown, protective oxide scale. If compared with ceramic interconnect, the metallic interconnect can reduce the fabrication cost, facilitate the production of more complex fuel cell designs and improve the efficiency of the fuel cell (Benjamin, 2004). Metallic material such as iron, nickel and cobalt based alloys are usually used in high temperature environment. Developing alloys metal with chromium, aluminium and silicon encourage the formation of protective oxide (scales) of chromia,

alumina and silica respectively. However, the protective oxide (scales) of alumina is low electrical conductivity as the performance loss (voltage loss across the insulating alumina scale) (Quadackers *et al.*, 2003). Iron (Fe) as metallic interconnect has many advantages such as good work ability, low cost and thermal expansion coefficient similar with other cell component. The chromium is formed on the surface during vaporization operation and decreasing the cathode activity. Nearly of all metallic materials as interconnect candidates are chromium forming alloy since the high electrical conductivity is provided by oxide Cr_2O_3 scale which is compared with Al_2O_3 and SiO_2 . However, the Chromium based alloys have some weakness such as formation of volatile Cr (VI) which is occur under operating environment SOFC. The migration of volatile Cr (VI) may occur and it poisons the cathode. The degradation of stack performance is over long term temperature (Jong-Hee Kim *et al.*, 2004). Therefore, there are several studies which are related to the FeCr alloy as metallic interconnect for high temperature SOFC and the modification for improving the conductivity of oxide scale is required (Jong-Hee Kim *et al.*, 2004). Fe-16Cr alloys (SUS430) have been studied on oxidation kinetics under the condition of the air and fuel side environments in SOFC application (Hideto *et al.*, 2004). The growth rate scale in the air and fuel side is almost same when reach of the temperature of 1073 K (Hideto *et al.*, 2004). In the air side, the growth rate of iron oxide is higher than in the steam side. It might be caused the hydrogen permeates from the effect of oxidation behaviour in steam side. Interconnect of SOFC is exposed simultaneously both of air and full atmospheres.

Ni-based alloy Haynes 242 with low coefficient of thermal expansion (CTE) was used as metallic interconnect by Geng *et al.*, (2006). They found that the parabolic law and weight gain of the alloy increased with the increase in oxidation temperature. In outer layer of NiO and an inner layer of Cr_2O_3 with $(\text{Mn,Cr})_3\text{O}_4$ observe that the oxide formed on it consisted but in the top NiO layer did not uniformly cover the surface. They also study the Ebrite and Haynes 230 alloy material for interconnect application. Commercial Ni-Cr based alloys divide to three i.e. Haynes 230, Hastelloy S and Haynes 242 used to evaluate the oxidation behaviour, scale conductivity and thermal expansion (Zhenguo Yang *et al.*, 2006). They found that the Haynes 230, Hastelloy S formed thin scale mainly comprised of Cr_2O_3 and $(\text{Mn,Cr,Ni})_3\text{O}_4$ spinel, excellent oxidation

resistance and high electrical conductivity while the Haynes 242 indicating limited oxidation resistance for interconnect application. Three alloys above possess a coefficient of thermal expansion (CTE) that is higher than Crofer 22 APU as candidate ferritic stainless steel.

This study focuses on the improving FeCr properties such as high thermal stability, reducing the crystallite size, more homogenous particle size and finer surface morphology of the material by using combination process. The summaries of the description of the metallic materials for interconnect are listed in Table 2. 7.

Table 2. 7 Varies metallic candidate material for interconnect application

No.	Author	Metallic material for interconnect	Analyzed to
1	Deni, 2011 and Hendi, 2011 Ade, 2012	Fe ₈₀ Cr ₂₀ FeCrAl	<ul style="list-style-type: none"> Investigate the crystallite size, oxidation kinetics, CTE, electrical properties, morphology and composition analysis. The distribution particle size, morphology, and oxidation kinetics.
2	Quadackers <i>et al.</i> , 2003	MnCrAl	Investigate the excellent oxidation protection of the alumina scale
3	Jong-Hee Kim <i>et al.</i> , 2004	iron, nickel, cobalt, chromium, aluminium and silicon	Investigate the electrical conductivity.
4	<ul style="list-style-type: none"> Hideto <i>et al.</i>, 2004 Murugesan <i>et al.</i>, 1999 Rajeev <i>et al.</i>, 2013 	Fe-16Cr alloys (SUS430) Fe _{1-x} Cr _x Fe ₂₀ Cr Alloy	<ul style="list-style-type: none"> Investigate the oxidation kinetics Investigate the magnetism of nanocrystalline alloys Investigate the corrosion rate or corrosion resistance
5	Geng <i>et al.</i> , 2006	Ni-based alloy Haynes 242 and Ebrite and Haynes 230	Investigate the parabolic law and weight gain.
6	Zhenguo Yang <i>et al.</i> , 2006	Ni-Cr based alloys: Haynes 230, Hastelloy S and Haynes 242	Investigate the oxidation behaviour, scale conductivity and thermal expansion

2.3.1 Chromium based alloys

Chromium based alloys have a crystal structure of Body Centred Cubic (BCC) and are not considered as super alloys. Evaporation of chromium species occurs from the protective Cr_2O_3 layer and the poisoning effects of these species occur at the electrolyte interface (Bastidas, 2006).

Chromium-based alloys were initially developed as a replacement of ceramic interconnects for electrolyte-supported planar SOFC. They are favoured because they have high oxidation resistance and fairly good corrosion resistance are provided by the formation of Cr_2O_3 scale in the presence of oxidant. The binary metal oxide Cr_2O_3 has large electronic conductivity (Zhong *et al.*, 2003 and Yang *et al.*, 2004). Thicker corrosion scales grow in the carbon-containing atmosphere (methane, propane, Liquefied Petroleum Gas (LPG) and coal gas) due to the formation of carbides (Bastidas, 2006). According to Zhu Wei-zhong, Yan Mi, (2004) that the Cr based alloys have main weakness as metal interconnect i.e. high oxidation level and developing Cr (VI) gas species which is easy to volatilize at the fuel cell operating temperature. The further oxidations of the Cr_2O_3 scale usually occur at the higher oxygen partial pressure in the end of the cathode prior to the electrochemical reduction of the oxygen. The Cr based alloys of this research have several properties that influence the result of the research. Material properties of Cr powder can be seen in Table 2. 8 (John Emsley, 2011b):

Table 2. 8 Properties of chromium powder (John Emsley, 2011b)

Properties		
Atomic number		24
Atomic mass		51,996
Melting point		1 900 °C / 2 173 K
Boiling point		2 672 °C / 2 945 K
Atomic volume		$1.2 \cdot 10^{-29} \text{ [m}^3\text{]}$
Vapor pressure	at 1 800 °C	267 [Pa]
	at 2 200 °C	7161 [Pa]
Density at 20 °C (293 K)		7.15 [g/cm ³]

REFERENCE

- Abdellaoui M. and E. Gaffet. (1996). The physics of mechanical alloying in a modified horizontal rod mill: Mathematical Treatment. *Acta mater.* Vol. 44, No. 2, pp. 125-134.
- Abdoli H., H. Farnoush, E. Salahi, K. Pourazrang. (2008). Study of the densification of a nanostructured composite powder Part 1: Effect of compaction pressure and reinforcement addition. *Materials Science and Engineering A*, 486, pp. 580–584.
- Ade Firdianto. (2012). *Ultrasonic treatment with nickel electroplating combined with oxidation for developing gamma alumina washcoat on Fe-Cr-Al substrate.* Universiti Tun Hussein Onn Malaysia, Malaysia: Master Thesis.
- Akira Terayama, Hideki Kyogoku, Masaru Sakamura and Shinichiro Komatsu. (2006). Fabrication of TiNi powder by mechanical alloying and shape memory characteristics of the sintered alloy. *Materials Transactions*, Vol. 47, No. 3, pp. 550-557.
- Alireza Nouri, and Cuie Wen. (2014). Surfactants in mechanical alloying/milling: A catch-22 situation. *Critical Reviews in Solid State and Materials Sciences.* Vol 39, pp. 81–108.
- Allen W. Burton, Kenneth Ong, Thomas Rea, Ignatius Y. Chan. (2009). On the estimation of average crystallite size of zeolites from the Scherrer equation: A critical evaluation of its application to zeolites with one-dimensional pore systems. *Microporous and Mesoporous Materials*, 117, pp. 75–90.
- ASM Handbook Vol. 3. (1992). *Alloy Phase Diagrams.* Materials Park, OH: ASM International.
- Baig A. A., J. L. Fox, R. A. Young, Z. Wang, J. Hsu, W. I. Higuchi, A. Chhetry, H. Zhuang, M. Otsuka. (1999). Relationships Among Carbonated Apatite